Since January 2020 Elsevier has created a COVID-19 resource centre with free information in English and Mandarin on the novel coronavirus COVID-19. The COVID-19 resource centre is hosted on Elsevier Connect, the company's public news and information website.

Biosensors and Bioelectronics 227 (2023) 115169

Contents lists available at ScienceDirect

Biosensors and Bioelectronics

journal homepage: www.elsevier.com/locate/bios

The SpACE-CCM: A facile and versatile cell culture medium-based biosensor for detection of SARS-CoV-2 spike-ACE2 interaction

Youngwook Ham [a,b], Nam-Chul Cho [c], Daeyong Kim [a,b], Jung-Hee Kim [d], Min Ju Jo [a,e], Min Seon Jeong [a,b], Bo-Yeong Pak [d], Sanghyeok Lee [d], Mi-Kyung Lee [f,g,h], Seung-Wook Chi [f,h], Tae-Don Kim [i,j], Nak Cheol Jeong [d], Sungchan Cho [a,b,*]

[a] Nucleic Acid Therapeutics Research Center, Korea Research Institute of Bioscience and Biotechnology (KRIBB), Cheongju, Chungbuk, 28116, Republic of Korea
[b] Department of Biomolecular Science, KRIBB School of Bioscience, Korea University of Science and Technology (KUST), Daejeon, 34113, Republic of Korea
[c] Korea Chemical Bank, Korea Research Institute of Chemical Technology (KRICT), Daejeon, 34114, Republic of Korea
[d] AM Science Corp., Gyeonggi, 12902, Republic of Korea
[e] College of Pharmacy, Chungbuk National University, Chungbuk, 28644, Republic of Korea
[f] Disease Target Structure Research Center, Korea Research Institute of Bioscience and Biotechnology (KRIBB), Daejeon, 34141, Republic of Korea
[g] Critical Diseases Diagnostics Convergence Research Center, Korea Research Institute of Bioscience and Biotechnology (KRIBB), Daejeon, 34141, Republic of Korea
[h] Department of Proteome Structural Biology, KRIBB School of Bioscience, Korea University of Science and Technology (KUST), Daejeon, 34113, Republic of Korea
[i] Immunotherapy Research Center, Korea Research Institute of Bioscience and Biotechnology (KRIBB), Daejeon, 34141, Republic of Korea
[j] Department of Functional Genomics, KRIBB School of Bioscience, Korea University of Science and Technology (KUST), Daejeon, 34113, Republic of Korea

ARTICLE INFO

Keywords:
COVID-19
SARS-CoV-2
Spike receptor-binding domain
ACE2
Protein-protein interaction
Cell culture medium-based biosensor

ABSTRACT

The COVID-19 pandemic is an ongoing global public health threat. COVID-19 is caused by severe acute respiratory syndrome coronavirus 2 (SARS-CoV-2) infection, and binding of the SARS-CoV-2 spike to its receptor, angiotensin-converting enzyme 2 (ACE2), on host cells is critical for viral infection. Here, we developed a luminescent biosensor that readily detects interactions of the spike receptor-binding domain (RBD) and ACE2 in cell culture medium ('SpACE-CCM'), which was based on bimolecular complementation of the split nanoluciferase-fused spike RBD and ectodomain of ACE2 and further engineered to be efficiently secreted from cells by adding a heterologous secretory signal peptide (SSP). Screening of various SSPs identified 'interferon-α+alanine-aspartate' as the SSP that induced the highest activity. The SpACE-CCM biosensor was validated by observing a marked reduction of the activity caused by interaction-defective mutations or in the presence of neutralizing antibodies, recombinant decoy proteins, or peptides. Importantly, the SpACE-CCM biosensor responded well in assay-validating conditions compared with conventional cell lysate-based NanoLuc Binary Technology, indicating its advantage. We further demonstrated the biosensor's versatility by quantitatively detecting neutralizing activity in blood samples from COVID-19 patients and vaccinated individuals, discovering a small molecule interfering with the spike RBD-ACE2 interaction through high-throughput screening, and assessing the cross-reactivity of neutralizing antibodies against SARS-CoV-2 variants. Because the SpACE-CCM is a facile and rapid one-step reaction biosensor that aptly recapitulates the native spike-ACE2 interaction, it would be advantageous in many experimental and clinical applications associated with this interaction.

1. Introduction

COVID-19 is a serious infectious disease that is causing an unprecedented threat to global public health, with the cumulative number of deaths worldwide exceeding 6.8 million as of January 2023, and its threat is still ongoing. It is caused by infection with severe acute respiratory syndrome coronavirus 2 (SARS-CoV-2). SARS-CoV-2 is an enveloped, single-stranded, positive-sense RNA virus with a genome size of approximately 30 kb and belongs to the β-coronavirus genus in the Coronaviridae family (Pal et al., 2020), which also includes viruses such as SARS-CoV and MERS-CoV, which can cause severe acute respiratory illness. SARS-CoV-2 is the most recently emerged coronavirus and has

* Corresponding author. Nucleic Acid Therapeutics Research Center, Korea Research Institute of Bioscience and Biotechnology (KRIBB), Cheongju, Chungbuk, 28116, Republic of Korea.
E-mail address: sungchan@kribb.re.kr (S. Cho).

https://doi.org/10.1016/j.bios.2023.115169
Received 17 November 2022; Received in revised form 5 February 2023; Accepted 17 February 2023
Available online 19 February 2023

the highest infectivity among coronaviruses, leading to increased mortality, particularly in older adults.

In the early stage of the COVID-19 pandemic, careful surveillance and epidemiological investigation of COVID-19 were critically required to limit the spread of SARS-CoV-2, reduce morbidity and mortality, and eventually end the COVID-19 emergency worldwide. As a result of enormous efforts, numerous diagnostic tools detecting viral RNAs or antigens were successfully developed, and some have been widely used for the diagnosis of COVID-19 (Carter et al., 2020). They include biosensors based on gold nanoparticles, magnetic nanoparticles, or clustered regularly interspaced short palindromic repeats (CRISPR) technology and enable rapid and sensitive detection of viral RNAs or antigens (Anik et al., 2021; Mahmud et al., 2022). As the COVID-19 pandemic has persisted and a considerable portion of the population has been vaccinated, diagnostic tools that detect neutralizing antibodies generated by SARS-CoV-2 infection or vaccination are additionally needed. Moreover, the continuous advent of new variants has also prompted the development of new diagnostic tools to assess the activity of protective neutralizing antibodies and their cross-reactivity against virus variants.

The spike protein and its interaction with the angiotensin-converting enzyme 2 (ACE2) protein on host cells, which are critical for the first step of viral infection, have drawn particular attention because the spike protein is a major target of protective neutralizing antibodies that form in convalescent patients and vaccinated individuals. Most efficacious neutralizing antibodies target the receptor-binding domain (RBD) of the spike protein, which is sufficient for binding to ACE2, and blocks the binding of the spike to ACE2 (Gattinger et al., 2022). This interaction is also considered a promising therapeutic target for the development of effective antivirals based on various modalities, such as therapeutic neutralizing antibodies, peptides, small molecules, or protein decoys.

Many different methods, including the plaque reduction neutralization test, surface plasmon resonance, and enzyme-linked immunosorbent assays (ELISAs), have been used to analyze the spike-ACE2 interaction, but they require a specialized facility with biosafety level (BSL) II or III and a high-level technique and are labor-intensive and time-consuming. To overcome these limitations, the nanoluciferase-based bioluminescence assay platform, i.e., NanoLuc Binary Technology (NanoBiT), was applied by several groups to analyze the spike-ACE2 interaction (Alves et al., 2021; Azad et al. 2021a, 2021b; Brown et al., 2021; Yang et al., 2021). In the NanoBiT assay, the nanoluciferase enzyme is split into two fragments, an 18-kDa large fragment (LgBiT) and an 11-amino acid small fragment (SmBiT), and each fragment is fused with a target protein of interest. The protein-protein interaction (PPI) of the spike and ACE2 leads to the physical reassembly of the LgBiT and SmBiT, resulting in complementing nanoluciferase activity and generating a luminescent signal. Because the NanoBiT assay is based on bimolecular luminescence complementation, it enables a simple, quantitative, and highly sensitive measurement that is amenable to high-throughput screening (HTS).

For instance, Yang et al. introduced the spike RBD and ACE2 into the NanoBiT system (Yang et al., 2021) and analyzed their interaction mainly using cell lysates. Azad et al. reported a similar approach, but they used the spike S1 protein instead of the spike RBD (Azad et al., 2021a). Alves et al. modified the conventional NanoBiT system so that bimolecular luminescence complementation occurred through antibody mediation and performed the assay using purified recombinant protein components (Alves et al., 2021). Most previously reported methods utilized intracellular protein sources by preparing either pure recombinant proteins or crude lysates from cells. Therefore, they required a delicate and complicated protein purification process or might not be optimal for the detection of extracellular PPIs such as the spike-ACE2 interaction, which requires glycosylation or other processes to completely recapitulate the native PPI.

The objective of our study was to develop a biosensor that accurately recapitulates the native interaction of the SARS-CoV-2 spike RBD and ACE2 and easily detects this interaction. To achieve this purpose, we modified the conventional NanoBiT biosensor to be efficiently secreted from mammalian cells by adding a heterologous secretory signal peptide (SSP) and consequently established a new biosensor that detected the spike RBD-ACE2 interaction in cell culture medium (SpACE-CCM) rather than in cell lysates or living cells. Its robustness was clearly demonstrated by both molecular and pharmacological methods. The optimized biosensor is convenient because it can perform assays in a single step. Importantly, comparative analyses showed that the SpACE-CCM biosensor recapitulates the actual interaction much better than the conventional NanoBiT biosensor, which mainly detects intracellular PPIs. Its usefulness was demonstrated in several relevant settings. The SpACE-CCM biosensor will be useful in many experimental and clinical applications such as monitoring neutralizing antibodies in populations, discovering therapeutic agents from HTS, and assessing cross-reactivity against variants.

2. Materials and methods

2.1. Cell culture and transfection

Human embryonic kidney 293T cells were maintained in Dulbecco's modified Eagle's medium (Welgene, Gyeongsangbuk-do, Republic of Korea, Cat.# LM 001–05) containing 10% fetal bovine serum (Welgene, Cat.#S001-01) and supplemented with 1% penicillin and streptomycin (Gibco, MD, USA, Cat.# 15140122). The 293T cells were seeded into six-well culture plates and maintained overnight. When the cells reached 60–80% confluence, they were transfected with biosensor plasmids using the X-tremeGENE Transfection Reagent (Roche, Basel, Switzerland, Cat.# 04476115001), according to the manufacturer's instructions. The X-tremeGENE Transfection Reagent is a multi-component reagent that forms a complex with DNA and transports the complex into mammalian cells with high efficiency and low cytotoxicity. Transfected cells were incubated at 37 °C for 48 h before harvesting.

2.2. Plasmid construction

A codon-optimized nucleotide sequence for the spike RBD (aa 319–541) of wild-type SARS-CoV-2 (Wuhan-Hu-1) was generated using the OptimumGeneTM algorithm and synthesized by GenScript (NJ, USA). DNA fragments encoding the ACE2 ectodomain (aa 18–740) were obtained by polymerase chain reaction (PCR) using a cDNA library of human MKN-74 cells. The resulting spike RBD and ACE2 ectodomain genes were separately cloned into pBiT1.2-N, pBiT1.2-C, pBiT2.2-N, and pBiT2.2-C vectors (Promega, WI, USA, Cat.#N2014), enabling LgBiT- or SmBiT-fused protein expression in mammalian cells. SSPs were additionally cloned into the N-terminal ends of the LgBiT-spike RBD and SmBiT-ACE2 proteins, and their nucleotide and amino acid sequences are listed in Table S1. Spike RBD and ACE2 mutations and spike RBD (Delta) genes were introduced using overlap extension PCR cloning (Cosmogenetech, Daejeon, Republic of Korea). SARS-CoV-2 variant genes (BA.1 and BA.5) were purchased from Addgene (MA, USA, Cat.# 185452, 186031) and subcloned into a pBiT1.2-N vector.

2.3. Western blot analysis

Whole-cell extracts were prepared and subjected to western blot analysis with the appropriate antibodies as described previously (Choi et al., 2021). Anti-spike RBD (1:1000, Sino Biological, Beijing, China, Cat.# 40592-T62), anti-ACE2 (1:1000, Abcam, Cambridge, UK, Cat.# ab108252), anti-glyceraldehyde-3-phosphate dehydrogenase (GAPDH) (1:5000, Santa Cruz Biotechnology, CA, USA, Cat.# sc-51905), anti--mouse (1:5000, Santa Cruz Biotechnology, Cat.# sc-516102), and anti-rabbit (1:5000, Enzo Biochem, NY, USA, Cat.# ADI-SAB-300-J) antibodies were used. Signals were detected on an Amersham™ Imager 680 (Amersham Bioscience, Buckinghamshire, UK) using a

Clarity™ Western ECL Substrate (Bio-Rad, CA, USA, Cat.# 170–5061).

2.4. NanoBiT assays in the total preparation, cell culture medium, and cells

To analyze NanoBiT activity in the total preparation, cell culture medium, and cells, 293T cells were transfected pairwise with the appropriate plasmids using the X-tremeGENE Transfection Reagent in 96-well plates (2×10^4 cells/well). Forty-eight hours after transfection, the total preparation, cell culture medium, and cell lysates were separately prepared as follows. To analyze NanoBiT activity in the total preparation, transfected cells maintained in 100 μl of cell culture medium were analyzed by directly adding the Nano-Glo Live reagent (Promega, Cat.#N1120) to each well as per the manufacturer's protocol. The Nano-Glo Live reagent is a non-lytic detection reagent used to measure NanoBiT activity from living cells. The luminescence was measured using a microplate reader (TECAN, Zurich, Switzerland). To analyze NanoBiT activity in the cell culture medium, medium was obtained from each well, and cells and cellular debris were removed by centrifugation at 1766 g for 5 min. Then, 100 μl of supernatant was transferred to another well in a 96-well plate and assayed by adding the Nano-Glo Live reagent. To analyze NanoBiT activity in cells, the whole-cell culture medium was first removed, and then the cells attached to the bottom were washed once with 1 × phosphate-buffered saline (PBS, pH 7.2). Thereafter, 100 μl of PBS was added, and the assay was conducted by adding the Nano-Glo Live reagent. To determine the optimal SSP, 293T cells were transfected pairwise with plasmids encoding fusion proteins tagged with various SSPs at their N-terminal ends and the firefly luciferase-expressing plasmid using the X-tremeGENE Transfection Reagent in 96-well plates (2×10^4 cells/well). Firefly luciferase gene expression was used to monitor the transfection efficiency. Forty-eight hours after transfection, the luciferase activity in the cell culture medium was measured using both the Nano-Glo Live and One-Glo Luciferase Assay Systems (Promega, Cat.#E6120 for the One-Glo System). The results are presented as the relative luciferase activity after normalization of the nanoluciferase activity to the corresponding firefly luciferase activity. The data were obtained from three independent experiments.

2.5. Optimization of the SpACE-CCM biosensor reaction conditions

To determine the optimal temperature, incubation time, and input amount for the SpACE-CCM biosensor reaction, 293T cells were transfected with plasmids encoding human interferon-α appended with alanine-aspartate (hIFNα+AD)-tagged LgBiT-spike RBD and SmBiT-ACE2 using the X-tremeGENE Transfection Reagent. Forty-eight hours after transfection, the cell culture medium was harvested and centrifuged at 1766 g for 5 min to remove cells and cellular debris. The supernatant, which is the source of the SpACE-CCM biosensor, was dispensed into a 96-well plate (100 μl/well) and incubated at 4, 15, 20, 25, 30, and 37 °C for various times. The luciferase activity was subsequently measured using the Nano-Glo Live reagent. The optimal amount of the supernatant for the SpACE-CCM biosensor was also determined. The supernatant was dispensed into a 96-well plate in a dose-dependent manner (0, 1, 3, 10, 30, and 100 μl/well), and the supernatant prepared from untransfected cells was added to make the final volumes equal (100 μl/well). The reaction mixture was incubated at 25 °C for 1 h, and the nanoluciferase activity was measured. To further determine the optimal reaction time, 10 μl of the supernatant was incubated with neutralizing antibodies, 40591 (Sino Biological, Cat.# 40591-MM43) and 40592 (Sino Biological, Cat.# 40592-MM57), at 1 and 10 μg/ml at 25 °C for 0, 5, 10, 20, 40, 60, and 90 min. IgG (GenScript, Cat.# A01007) and 1A9 (GeneTex, TX, USA, Cat.# GTX632604) antibodies were used as negative controls.

2.6. Pharmacological validation of the SpACE-CCM biosensor using neutralizing antibodies, peptides, and recombinant proteins

To validate the SpACE-CCM biosensor in pharmacological assays, the inhibitory activity of neutralizing antibodies, peptides, and recombinant spike RBD and ACE2 proteins was assessed using the optimized SpACE-CCM assay. The SpACE-CCM biosensor was prepared as described in the 'Optimization of the SpACE-CCM biosensor reaction conditions' section, and 10 μl of cell culture medium was incubated with the 40591, 40592, 6D11F2 (GenScript, Cat.# A02055), and AM001414 (ActiveMotif, CA, USA, Cat.# 91361) recombinant neutralizing antibodies at 0.1, 0.3, 1, 3, and 10 μg/ml at 25 °C for 1 h. IgG and 1A9 antibodies were used as negative controls. Similarly, the SpACE-CCM biosensor activity was evaluated in the presence of peptides (LCB2 and LCB4, synthesized by GenScript) and the recombinant spike RBD (aa 319–541, Raybiotech, GA, USA, Cat.# 230–30162) or ACE2 (aa 18–740, Raybiotech, Cat.# 230–30165) proteins.

2.7. Long-term storage evaluation of the SpACE-CCM biosensor

To evaluate the stability of the SpACE-CCM biosensor according to the storage period, three types of cell culture media were prepared on different days and stored at −20 °C for up to 1 year. Frozen cell culture medium was thawed at room temperature for 30 min and transferred to a 96-well plate, and the nanoluciferase activity was measured. Additionally, to evaluate the responsiveness of the SpACE-CCM biosensor, 10-μl samples stored for 1 year were incubated with the recombinant neutralizing antibodies (40591 and 40592) at 0.1, 0.3, 1, 3, and 10 μg/ml at 25 °C for 1 h, and the nanoluciferase activity was measured using the Nano-Glo Live reagent. The IgG antibody was used as a negative control.

2.8. Assessment of neutralizing antibodies in clinical samples using the SpACE-CCM biosensor

Sera of convalescent COVID-19 patients (Cat.# CoV-Neut-S-100), vaccinated individuals (Moderna: Cat.# CoV-NVM1-S-100 and Pfizer-BioNTech: Cat.# CoV–NVP1–S-100), and healthy people (Cat.# NEGSMPL-S-100) were purchased from Raybiotech. Individuals who had been neither infected with SARS-CoV-2 nor vaccinated were regarded as healthy individuals, and these samples were obtained before the COVID-19 outbreak. Serially diluted sera were pre-incubated with cell culture medium containing the LgBiT-spike RBD at 25 °C for 30 min, and cell culture medium containing SmBiT-ACE2 was added and incubated for 10 min. Thereafter, the nanoluciferase activity was measured using the Nano-Glo Live reagent.

2.9. ELISA-based spike RBD-ACE2 binding assay

Sera containing neutralizing antibodies and small molecules that inhibited the spike RBD-ACE2 interaction were also analyzed using a SARS-CoV-2 Spike:ACE2 Inhibitor Screening Assay Kit (BPS Bioscience, CA, USA, Cat.# 79931), according to the manufacturer's instructions. Diluted sera of convalescent patients and vaccinated individuals were used to evaluate the correlation of responsiveness between the SpACE-CCM biosensor and an ELISA. Small molecules were added at a concentration of 50 μM and incubated at 25 °C for 1 h, and IgG and 40592 antibodies (10 μg/ml) were included as positive controls. The luminescence, which indicated spike RBD-ACE2 binding activity, was measured using a microplate reader, according to the manufacturer's instructions.

2.10. Virtual screening, SpACE-CCM-based screening, and molecular docking of spike RBD-ACE2 PPI small molecule inhibitors

Virtual screening of the chemical library of the Korea Chemical Bank (KCB, 677,730 compounds) was performed by molecular docking

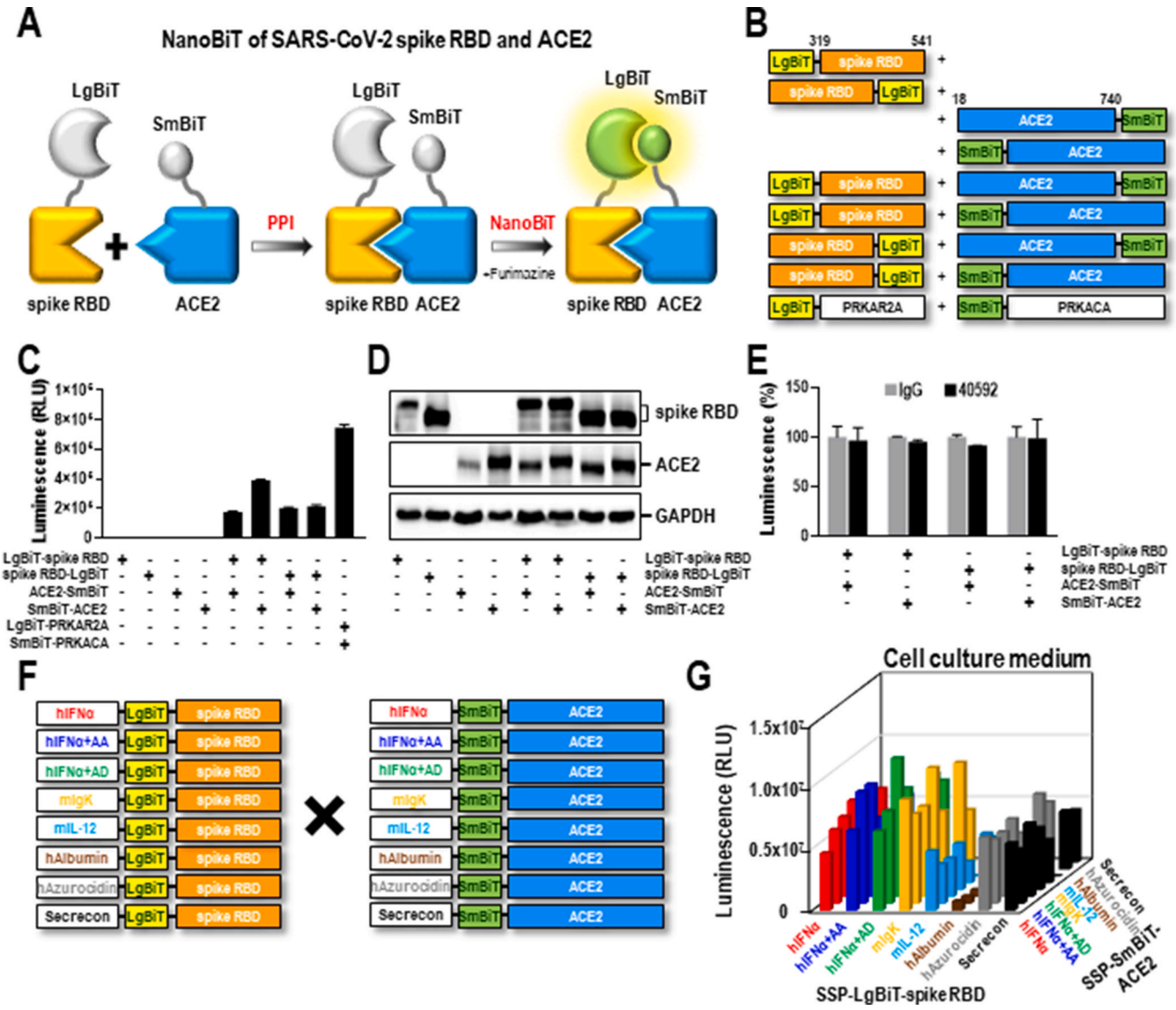

Fig. 1. Development of a secreted NanoBiT-based biosensor for detection of the spike RBD-ACE2 interaction. (A) Schematic of the SARS-CoV-2 spike RBD-ACE2 NanoBiT biosensor. (B) Configurations of the LgBiT-spike RBD (aa 319–541) and SmBiT-ACE2 (aa 18–740, without the native SSP). (C) Various NanoBiT configuration pairs were assessed by measuring the nanoluciferase activity in living cells (n = 3 biological replicates, mean ± SD). (D) Western blot analysis of the spike RBD and ACE2 fusion proteins expressed in 293T cells. (E) Responsiveness of NanoBiT assays to a spike RBD-neutralizing antibody. Cell lysates (10 μg) containing the spike RBD and ACE2 fusion proteins were incubated with the 40592 antibody (1 μg/ml) at 25 °C for 1 h, and the nanoluciferase activity was measured. (F) The indicated SSPs were fused to the N-terminal ends of both LgBiT-spike RBD and SmBiT-ACE2. (G) Identification of an optimal SSP for efficient secretion. Results are presented as the nanoluciferase activity normalized to the firefly luciferase activity.

simulation and shape screening using Schrodinger's program. This program provides various tools that facilitate the investigation of virtual modeling of small molecules using molecular docking simulations and molecular dynamic simulation modules (Friesner et al., 2004). A linoleic acid (LA)-bound SARS-CoV-2 spike glycoprotein structure (protein data bank code: 6ZB4) was downloaded from the Research Collaboratory for Structural Bioinformatics (RCSB) database. Chains A and C of the LA-binding site on the spike RBD were prepared by protonation at pH 7.4 and energy minimization. A grid for molecular docking simulation was created around the LA-binding site with 10 Å spacing, and the KCB chemical library was screened using the Glide SP module. The binding conformation of LA in the spike RBD was used as a query for shape screening with three volume scores (typed pharmacophore, typed atoms, and untyped atoms). In total, 30,000 compound outputs obtained from shape screening docked to the LA-binding site. The virtual hits were prioritized by docking score, and 430 compounds were further chosen by visual inspection. Later, derivatives of the A09 compound were searched using the Instant JChem program, which supports substructure, similarity, superstructure, and exact searching of structure fields on individual datasets or databases (ChemAxon, 2017).

2.11. Cross-reactivity analysis of neutralizing antibodies against variants

Recombinant neutralizing antibodies were assessed for their cross-reactivity against various SARS-CoV-2 variants using the SpACE-CCM biosensor. SpACE-CCM biosensor constructs for three recent variants (Delta, BA.1, and BA.5) were generated, and their biosensors were separately prepared according to the procedure in the 'Optimization of the SpACE-CCM biosensor reaction conditions' section. The recombinant neutralizing antibodies 40591, 40592, 40150 (Sino Biological, Cat. # 40150-D001), BS-R2B2 (GenScript, Cat.# A02051), and BS-R2B17 (GenScript, Cat.# A02052) were used for the analysis. The

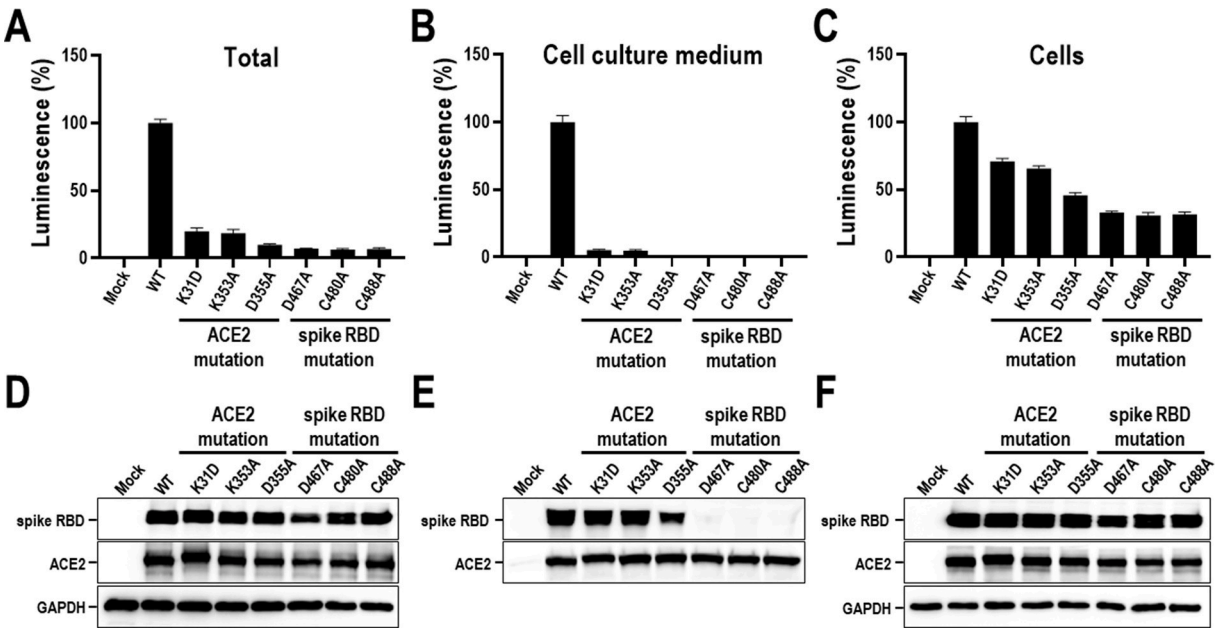

Fig. 2. Validation of the SpACE-CCM biosensor using PPI-defective mutations. SpACE-CCM biosensor components with the wild-type or six PPI-defective mutations as indicated were expressed in 293T cells, and the nanoluciferase activity in the (A) total preparation, (B) cell culture medium, and (C) cells were separately measured (n = 3 biological replicates, mean ± SD). In addition, protein samples were prepared from the (D) total preparation, (E) cell culture medium, and (F) cells and analyzed by western blotting with anti-spike RBD and -ACE2 antibodies. GAPDH was used as a loading control.

neutralizing antibodies were incubated with the SpACE-CCM biosensors of the wild-type virus and variants at 0.1, 0.3, 1, 3, and 10 μg/ml at 25 °C for 1 h, and the nanoluciferase activity was measured using the Nano-Glo Live reagent.

3. Results and discussion

3.1. Determination of the optimal NanoBiT configuration to detect spike RBD-ACE2 interactions

Because the spike RBD is a major target of neutralizing antibodies found in convalescent COVID-19 patients and is an optimal target for vaccination and immunotherapy (Min and Sun, 2021), we used the spike RBD as a counterpart of ACE2 to develop a facile and sensitive NanoBiT-based biosensor that could quantitatively detect the spike-ACE2 PPI. The spike RBD (aa 319–541) and ACE2 ectodomain (aa 18–740, lacking the native SSP, transmembrane domain, and intracellular domain), for which an efficient PPI was shown *in vitro* and in cells, were introduced into the NanoBiT system. Then, codon optimization was applied, particularly to the spike RBD sequence, to enhance the translational efficiency in mammalian cells. Considering the protein sizes of the spike RBD (approximately 25 kDa) and ACE2 ectodomain (approximately 84 kDa), the LgBiT was fused to the spike RBD, and the SmBiT was fused to the ACE2 ectodomain (Fig. 1A). Moreover, a glycine/serine-rich peptide was inserted between the spike RBD or ACE2 and LgBiT or SmBiT to allow a dynamic interaction and facilitate activity complementation of the split nanoluciferase. To determine the optimal fusion configuration of the spike RBD and ACE2 in the NanoBiT system, four fusion proteins (Fig. 1B) were expressed pairwise and assayed for their NanoBiT activities in living cells. As expected, all spike RBD-ACE2 NanoBiT pairs exhibited considerable nanoluciferase activity (2–4 × 10^5 relative light units, RLU), while a single component of the NanoBiT alone had little activity (2–8 × 10^2 RLU). The LgBiT-spike RBD and SmBiT-ACE2 configuration showed higher activity than that of other configuration pairs (Fig. 1C), even though the protein expression levels were similar (Fig. 1D). Of note, the highest NanoBiT activity was lower than that of the PRKACA-PRKAR2A PPI (approximately 8 × 10^5 RLU), the interaction between the catalytic subunit (PRKACA) and regulatory subunit (PRKAR2A) of protein kinase A (Varjosalo et al., 2013), which was used as the positive control. Because the relatively high NanoBiT activity of the LgBiT-spike RBD and SmBiT-ACE2 configuration pair may have resulted from a more efficient interaction than that of other configuration pairs, it was regarded as the optimal configuration pair for subsequent studies. To further validate the pharmacological utility, we applied an anti-spike RBD monoclonal antibody (40592), which has been shown to potently inhibit the interaction between the spike RBD and ACE2 and thus is prevalently used as a neutralizing antibody (Azad et al. 2021a, 2021b; Kim et al., 2022), to cell lysates prepared from cells expressing each configuration pair. Unexpectedly, the NanoBiT activity of all configuration pairs was barely affected by addition of the 40592 antibody at a sufficiently high concentration (1 μg/ml) (Fig. 1E), and even at a higher concentration (10 μg/ml), little effect was observed (Fig. S1A). Nevertheless, the neutralizing capability of the 40592 antibody was clearly demonstrated by its strong inhibitory effect on the spike RBD-ACE2 interaction in an ELISA (Fig. S1B). These results indicated the relatively low complementation activity and lack of pharmacological responsiveness of the preliminarily tested NanoBiT assays. In this system, spike RBD- and ACE2-fused proteins did not have an SSP at their N-terminal ends. Therefore, they were predicted to not be primarily directed to the secretory pathway and to not undergo the post-translational modification of glycosylation in the endoplasmic reticulum and Golgi complex, which is essential for extracellular proteins (including membrane proteins), especially for interactions such as the spike-ACE2 PPI. It should be noted that recent studies have revealed a critical contribution of spike RBD glycosylation to the interaction with ACE2 (Azad et al., 2021b; Li et al., 2020). Because these results collectively suggested the importance of SSPs for the intrinsic spike RBD-ACE2 interaction, we further included SSPs in the optimal configuration of the NanoBiT system.

3.2. Identification of an optimal SSP for the SpACE-CCM biosensor

To direct spike RBD- and ACE2-fused proteins to the secretory pathway and induce efficient secretion in the cell culture medium, we searched for SSPs through data mining. We selected those reported to have strong secretion-inducing activity in mammalian cells (Attallah

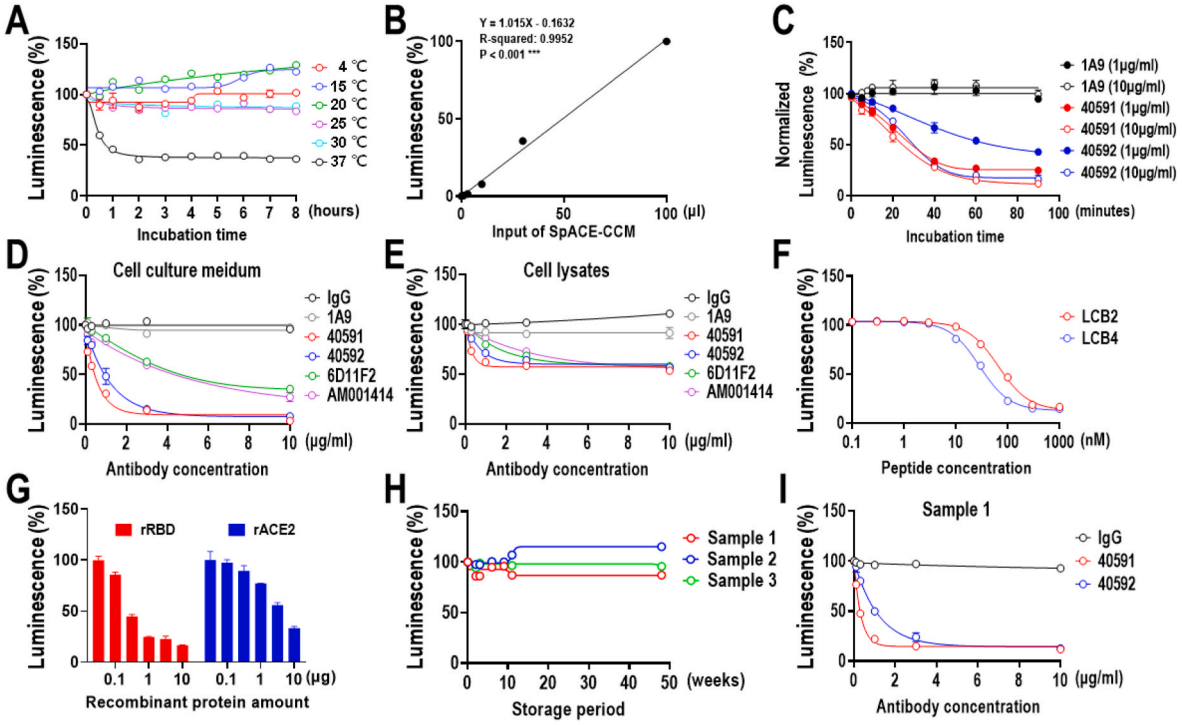

Fig. 3. Optimization and pharmacological validation of the SpACE-CCM biosensor. (A) The biosensor stability was analyzed at the indicated temperatures and incubation times (n = 3 biological replicates, mean ± SD). (B) Correlation analysis of the biosensor activity and the biosensor input amount. The correlation was calculated with Pearson's correlation coefficient using GraphPad Prism. Statistical significance was calculated using a two-tailed Student's t-test and presented as a *p*-value (****, $p < 0.001$). (C) The spike RBD-neutralizing antibodies 40591 and 40592 were incubated with 10 μl of the biosensor at 25 °C for the indicated times, and the biosensor activity was measured. (D) The biosensor (10 μl of the cell culture medium) and (E) an equivalent amount of cell lysate (10 μg) were incubated with the indicated concentrations of spike RBD-neutralizing antibodies, control IgG, and 1A9 antibody at 25 °C for 1 h, and the biosensor activity was measured. The PPI-inhibitory effects of (F) the LCB2 and LCB4 peptide inhibitors and (G) recombinant spike RBD and ACE2 proteins were evaluated with the biosensor. (H) Three biosensor samples stored at −20 °C were thawed at the indicated times, and their biosensor activity was measured. (I) Biosensor that had been stored for 1 year was incubated with IgG, 40591, and 40592 antibodies at 25 °C for 1 h, and the biosensor activity was measured.

et al., 2017; Cho et al., 2019; Guler-Gane et al., 2016; Kober et al., 2013; Liu et al., 2016; Roman et al., 2016) and introduced them into the N-terminal ends of both components of the NanoBiT system (Fig. 1F). Sixty-four possible combinations of selected SSPs were screened to identify a combination capable of inducing the highest secretion level in the cell culture medium. Among them, the combination including the human interferon-α SSP appended with alanine-aspartate (AD) at the C-terminus (hIFNα+AD), in both the LgBiT-spike RBD and SmBiT-ACE2, exhibited the highest NanoBiT activity in cell culture medium (Fig. 1G). Further analysis also showed that the hIFNα+AD combination exhibited greater NanoBiT activity than that of the native SSPs of the spike and ACE2 (Fig. S2). Moreover, the optimality of the LgBiT-spike RBD and SmBiT-ACE2 configuration was confirmed in the context of the hIFNα+AD addition because this combination produced the highest NanoBiT activity in the cell culture medium among four possible configuration pairs (Fig. S3). This engineered and optimized NanoBiT assay with the LgBiT-spike RBD and SmBiT-ACE2 configuration readily detected the spike RBD and ACE2 interaction in cell culture medium and was named the SpACE-CCM biosensor.

3.3. Molecular validation of the SpACE-CCM biosensor

A previous study identified several residues important for the spike RBD and ACE2 interaction (Azad et al., 2021b). To evaluate the molecular validity of the SpACE-CCM biosensor, we introduced several previously identified mutations that could disrupt the spike RBD and ACE2 interaction, each in the spike RBD (D467A, C480A, or C488A) and ACE2 (K31D, K353A, or D355A) of the biosensor, expressed them in 293T cells, and measured the biosensor activity in the cell culture media (for the SpACE-CCM biosensor) and in cell lysates and the total preparation (conventional assays for comparison). As shown in Fig. 2B, the cell culture media activity (SpACE-CCM biosensors) was dramatically reduced by all mutations compared with that of the wild-type. However, high levels of mutant proteins (especially ACE2 mutants) were detected, similar to the wild-type, strongly supporting that the luminescence of wild-type SpACE-CCM is produced by the specific interaction of the spike RBD and ACE2. In a comparative analysis, the cell lysate activity was much less affected by the same mutations than that in corresponding cell culture media (compare Fig. 2C and B). The total activity was simply the average of the cell culture media activity and the cell lysate activity (Fig. 2A). These results collectively demonstrated that our newly developed SpACE-CCM biosensor sensitively detected a specific interaction between the spike RBD and ACE2 and had the advantage of recapitulating the native PPI. Another intriguing observation from these experiments was the clear difference in spike RBD mutant levels between cell culture media and cell lysates (compare Fig. 2E and F). Unlike the low spike RBD mutant levels in cell culture media (Fig. 2E), considerable amounts of proteins in similar levels were detected in cell lysates (Fig. 2F), and slightly different levels were found in the total preparation (Fig. 2D), indicating that spike RBD mutants were expressed efficiently inside cells but produced little secretion or were easily degraded in cell culture media. This phenomenon could be explained by a possible contribution of the D467, C480, or C488 residues to post-translational processing, including glycosylation or protein degradation of the spike RBD.

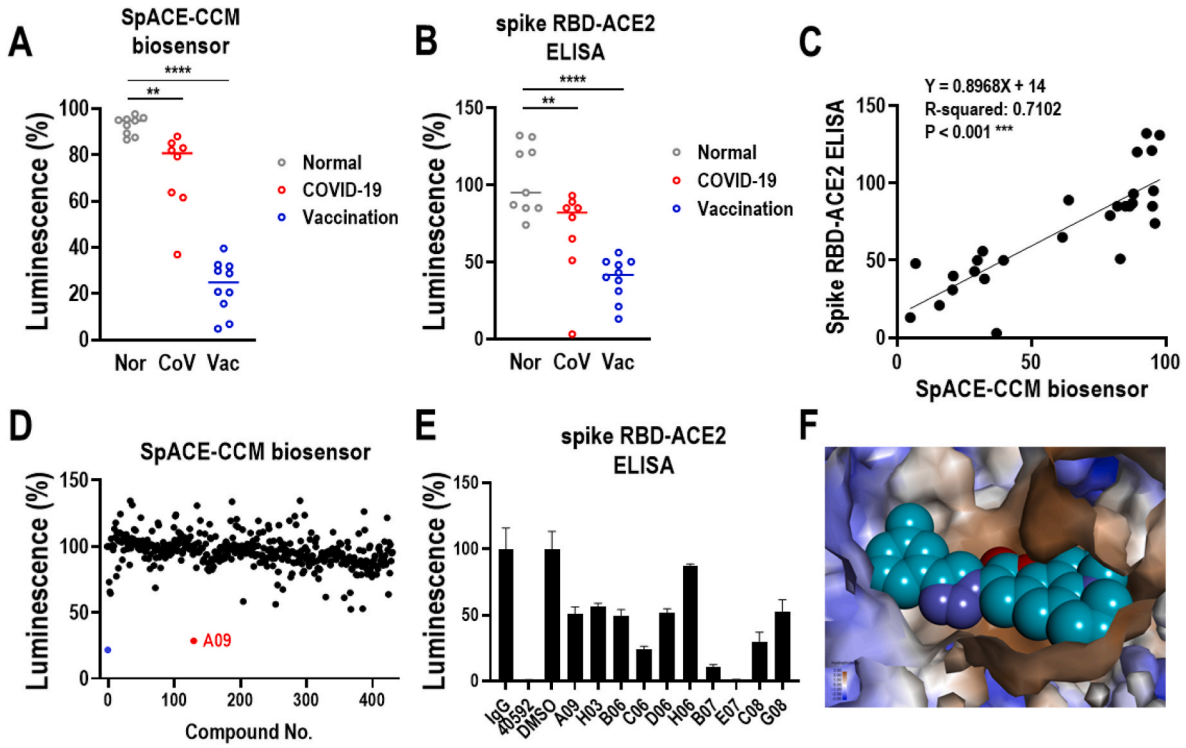

Fig. 4. Application of the SpACE-CCM biosensor for assessment of neutralizing antibodies in clinical samples and for the discovery of small molecule PPI inhibitors. Sera obtained from COVID-19 patients, vaccinated individuals, and healthy people were analyzed to determine their PPI-inhibitory activities using (A) the SpACE-CCM biosensor and (B) the conventional ELISA that detects the spike RBD-ACE2 interaction (n = 3 biological replicates, mean ± SD; one-way ANOVA, ****$p <$ 0.0001 and **$p < 0.01$ relative to normal, Dunnett's correction for multiple comparisons was performed using GraphPad Prism). (C) The neutralizing activity measured from the two assays is plotted on the graph, and their correlation was calculated with Pearson's correlation coefficient using GraphPad Prism. Statistical significance was calculated using a two-tailed Student's t-test and is shown as a *p*-value (****, $p < 0.001$). (D) HTS was performed to discover small molecule inhibitors of the spike RBD-ACE2 PPI using the SpACE-CCM biosensor. The spike RBD-neutralizing antibody 40592 was included as a positive control (blue dot). (E) The hit compound A9 and nine derivatives were further evaluated with the spike RBD-ACE2 PPI ELISA. (F) The predicted binding mode of compound E07 with the hydrophobic pocket in the spike RBD is shown in a space-filling diagram. The hydrophobic area around the pocket is shown in brown, and the hydrophilic area is shown in blue.

3.4. Optimization of the SpACE-CCM biosensor reaction and its pharmacological validation

We sought to optimize the SpACE-CCM biosensor reaction to utilize it for various purposes such as detection of spike-neutralizing antibodies from COVID-19 patients and discovery of spike-ACE2 PPI inhibitors. We primarily tested the stability of the biosensor according to temperature and incubation time and found that the biosensor activity was almost fully sustained at all tested temperatures, except for 37 °C, for up to 8 h, suggesting a facile reaction at room temperature (Fig. 3A). We then analyzed biosensor activity according to the amount of biosensor input and found a strong correlation between these two variables (R-squared value of 0.9952), indicating the quantitative feature of the biosensor (Fig. 3B). In addition, 10 μl of the biosensor was sufficient to produce a high luminescence readout (3×10^5 RLU). Next, we analyzed the dynamics of the biosensor in response to spike RBD-neutralizing antibodies according to the reaction time. The biosensor activity was decreased by incubation with the neutralizing antibodies 40591 and 40592 in a time-dependent manner, and their inhibitory effects reached maximum levels at approximately 1 h (Fig. 3C). As a negative control, a monoclonal antibody 1A9, which binds specifically to the S2 domain of the spike protein, had little effect on biosensor activity. According to these results, the optimal SpACE-CCM biosensor reaction condition was determined to be incubation of 10 μl of biosensor with the tested sample at 25 °C for 1 h. To further substantiate the pharmacological validity of the SpACE-CCM biosensor and assess its sensitivity, we utilized various PPI inhibitors such as neutralizing antibodies, peptides, and recombinant proteins, which could interfere with the spike RBD and ACE2 interaction. In the case of neutralizing antibodies, all tested antibodies decreased the biosensor activity in a dose-dependent manner, and the 40591 and 40592 antibodies exhibited stronger effects than the 6D11F2 and AM001414 antibodies (Fig. 3D). Particularly, the half maximal effective concentration (EC_{50}) of the 40591 antibody, which had the strongest effect, was estimated to be 0.2 μg/ml (corresponding to 1.33 nM). Overall, these results were consistent with the previous results obtained from ELISAs (Abe et al., 2020; Alves et al., 2021; Wan et al., 2020; Wu et al., 2022). In a comparative analysis, we observed that the same neutralizing antibodies also decreased the activity in cell lysates (conventional NanoBiT assay) but to a much lesser extent than that in cell culture media (SpACE-CCM biosensor) (compare Fig. 3D and E). This result is similar to the comparative results obtained from molecular validation experiments using PPI-defective mutations (Fig. 2B and C), supporting that our SpACE-CCM biosensor had an advantage in recapitulating the native extracellular PPI of the spike RBD and ACE2. A previous study reported small and stable peptides that tightly bind to the spike RBD and block its binding to ACE2 (Cao et al., 2020). 2020). We thus evaluated the effect of ACE2-mimetic peptides (LCB2 and LCB4) on SpACE-CCM biosensor activity and observed strong inhibition with an estimated EC_{50} of approximately 40–80 nM (Fig. 3F). The soluble recombinant spike RBD and ACE2, which could act as decoys and bind to components of the biosensor, were also evaluated under the same conditions and shown to considerably inhibit biosensor activity (Fig. 3G). Combined with the molecular validation experiment results (Fig. 2), these results clearly demonstrated not only the robustness of our SpACE-CCM biosensor as a tool to detect the specific interaction of the spike RBD and ACE2, but also its advantages in many aspects (easy

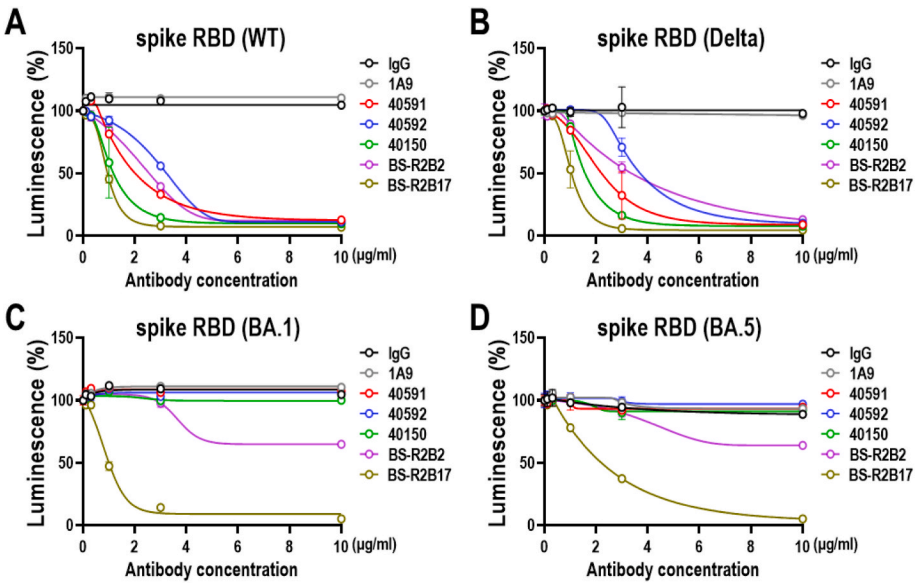

Fig. 5. Evaluation of the cross-reactivity of neutralizing antibodies with SARS-CoV-2 variants. (A) The wild-type and three major variants [(B) Delta, (C) BA.1, and (D) BA.5] of the spike RBD were introduced into the biosensor and were then used to evaluate the neutralizing antibodies at the indicated concentrations.

preparation, ultrasensitive, short reaction time, virus-free, one-step reaction, high specificity, high responsiveness, suitable for HTS, and cost-effectiveness). Moreover, we evaluated the long-term stability of the biosensor and observed that its activity was fully sustained even after storage at −20 °C for up to 1 year (Fig. 3H), after which time the stored biosensor retained its original level of reactivity to the neutralizing antibodies (Fig. 3I). These results indicate that the SpACE-CCM biosensor can be stored by general refrigeration instead of ultra-low temperature freezing for at least 1 year without loss of activity, which is an additional advantage of our biosensor system, especially for commercialization.

3.5. Detection of neutralizing activity in clinical samples from COVID-19 patients and vaccinated individuals

Based on the advantages of the SpACE-CCM biosensor, we examined its utility for various applications. First, to determine how well the biosensor can detect neutralizing antibodies in clinical samples, we applied sera obtained from convalescent COVID-19 patients and vaccinated individuals to the biosensor. Sera from healthy people were used as negative controls. Serially diluted sera from COVID-19 patients and vaccinated individuals significantly decreased the biosensor activity in a dose-dependent manner, and the decrease relative to that in healthy controls was largest at a 1 to 16 dilution (Fig. 4A). Intriguingly, sera from vaccinated individuals exhibited a stronger effect than that from COVID-19 patients. Nevertheless, these results do not indicate that neutralizing activity in vaccinated individuals is generally greater than that in patients naturally infected with SARS-CoV-2 because the titers and activities of neutralizing antibodies could vary depending on the incubation period of the infection, vaccination period, and number of vaccinations. To determine whether the SpACE-CCM biosensor properly responds to neutralizing antibodies, the same serum samples were analyzed using a conventional spike RBD-ACE2 PPI ELISA (Fig. 4B), and the results were compared with those from the biosensor assays. The neutralizing effects measured by the ELISA were similar to those from the biosensor assays, and the correlation of responsiveness between these two assays was significantly high as shown by an R-squared value of 0.7102 (Fig. 4C).

3.6. Application of the SpACE-CCM biosensor for the discovery of PPI inhibitors through HTS

A recent study reported the presence of a hydrophobic pocket on the spike RBD that can bind LA (Toelzer et al., 2020). According to the cryo-electron microscopy structure of spike RBD-bound LA complexed with ACE2 found in that study, the chemical structure of LA fits well with the bent hydrophobic pocket (Fig. S4), induces a closed conformation of the trimeric spike protein complex, and consequently interferes with the interaction with ACE2. Therefore, this hydrophobic pocket is considered a potential druggable target site for the development of COVID-19 treatments. To demonstrate the utility of the SpACE-CCM biosensor for the discovery of PPI inhibitors, we primarily performed a virtual screening of the KCB chemical library. All of the approximately 670,000 compounds were virtually screened by docking into the LA-binding pocket, and 430 compounds were finally selected as primary candidates. A more detailed procedure for compound selection is shown in the Materials and Methods. A second screening of 430 compounds was then carried out using the SpACE-CCM biosensor, and the A09 compound was identified as the strongest candidate, with inhibitory activity of approximately 75% compared with the DMSO control (Fig. 4D). Next, to confirm the PPI-inhibitory effect of A09 and determine whether any PPI inhibitors were more potent than A09, we chose nine additional compounds with a chemical structure similar to A09 and evaluated their PPI-inhibitory activities using the spike RBD-ACE2 ELISA. A09 inhibited the PPI activity by approximately 50% compared with the DMSO control, and C06, B07, and E07 were more effective than A09 (Fig. 4E). Particularly, E07 completely inhibited the spike RBD-ACE2 interaction, similar to the inhibitory effect of the neutralizing antibody 40592. Moreover, the binding mode of E07 in the hydrophobic pocket was predicted. E07, which is composed of tetracyclic coumarin, triazole, and phenyl rings, lined the LA-binding site and was stabilized by hydrophobic interaction with aromatic (Phe338, Phe342, Tyr365, Tyr369, Phe374, and Phe392) and aliphatic (Ala363, Leu368, Ile358, and Leu513) residues (Fig. S5). The tetracyclic coumarin moiety was fully filled in the hydrophobic part of the LA-binding site (Fig. 4F). These extensive interactions were also commonly found in docking poses of B07 and C06 (Fog. S6). Intriguingly, the *m*-methyl phenyl ring of E07 had a more favorable interaction with Tyr369 than that of the thiophene of B07 or the *m*-amino phenyl ring of C06 (Fig. S6), suggesting that this additional interaction might

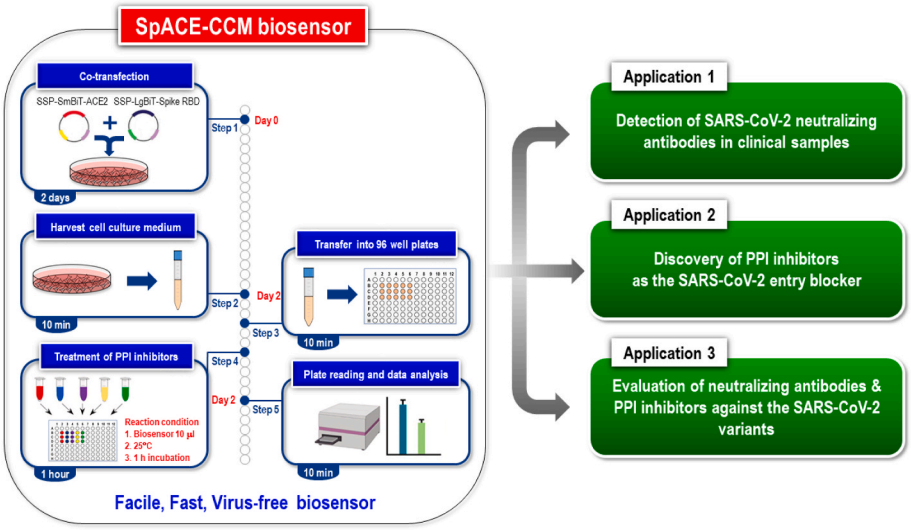

Fig. 6. Advantages of the SpACE-CCM biosensor and its usefulness for various applications. We engineered the conventional NanoBiT system and developed the SpACE-CCM biosensor, which readily detects the spike RBD and ACE2 interaction using cell culture medium and has several advantages described in the Conclusion section. This sensor could be useful for various applications associated with the spike RBD-ACE2 interaction such as (1) evaluation of neutralizing antibodies in clinical samples, (2) discovery of PPI inhibitors, and (3) evaluation of cross-reactivity against SARS-CoV-2 variants.

explain the greater inhibitory activity of E07 (Fig. 4E).

3.7. Assessment of cross-reactivity of the neutralizing activity against SARS-CoV-2 variants

Similar to other RNA viruses, SARS-CoV-2 is prone to genetic evolution as it adapts to new human hosts with the development of mutations over time, resulting in variants resistant to neutralizing antibodies of convalescent COVID-19 patients and vaccinated individuals (Tada et al., 2022). Since the initial advent of wild-type SARS-CoV-2 at the end of 2019, numerous variants with different infectivity, transmission ability, and pathology have continuously emerged, and subvariants of the Omicron variant are currently dominant as of the end of 2022 (Fan et al., 2022). Therefore, we chose four major variants of SARS-CoV-2 (wild-type, Delta, and Omicron BA.1 and BA.5), established each SpACE-CCM biosensor, and then evaluated the cross-reactivity of five neutralizing antibodies against these variants. All antibodies were effective for the wild-type, even though their effectiveness was somewhat variable with an EC_{50} of approximately 0.5–4 μg/ml (Fig. 5A). However, their inhibitory effects were weaker on the Delta variant than on the wild-type virus (Fig. 5B) and were weakest on the BA.1 and BA.5 variants (Fig. 5C and D). Nevertheless, it should be noted that the BS-R2B17 antibody solely exhibited a considerable inhibitory effect on all three variants and the wild-type. These results indicate that our biosensor would be a useful tool to evaluate the efficacy of neutralizing antibodies against newly emerging variants, especially for multiple combinations of antibodies and variants.

4. Conclusions

Our biosensor is easier to prepare than other methods, which require a delicate and complicated protein purification process, and it enables a rapid, ultrasensitive, and quantitative analysis (Fig. 3). The assay can be performed in basic laboratories and BSL-1 facilities and has no requirement for a higher BSL because it does not involve live viruses (Fig. 6). In addition, our biosensor is a convenient method in that its reaction can be performed in a single step with no further steps such as cell lysis, washing, and pre-incubation; however, pre-incubation generally increases its efficacy (Fig. 6). Moreover, the biosensor activity could be fully sustained at −20 °C for at least 1 year without loss of responsiveness, demonstrating its durability and suggesting the possibility of commercialization (Fig. 3H and I). Because the SpACE-CCM is a facile and cost-effective biosensor with multiple advantages, it would be useful for population-based massive surveys of neutralizing antibodies and for HTS of PPI inhibitors (Fig. 6). Its usefulness would be highlighted by application for assessment of the cross-reactivity of neutralizing antibodies and PPI inhibitors against newly emerging variants, especially in the multiplex format (Fig. 6). Beyond application for the spike RBD-ACE interaction, the cell culture medium-based NanoBiT assay will serve as a powerful technology platform for detection of PPIs among extracellular proteins (including membrane proteins).

CRediT authorship contribution statement

Youngwook Ham: Data curation, Formal analysis, Investigation, Methodology, Project administration, Validation, Visualization, Writing – original draft. **Nam-Chul Cho:** Data curation, Formal analysis, Methodology, Software, Visualization. **Daeyong Kim:** Data curation, Formal analysis, Investigation, Visualization. **Jung-Hee Kim:** Investigation, Formal analysis. **Min Ju Jo:** Investigation, Methodology. **Min Seon Jeong:** Investigation, Methodology. **Bo-Yeong Pak:** Investigation. **Sanghyeok Lee:** Investigation. **Mi-Kyung Lee:** Resources, Funding acquisition. **Seung-Wook Chi:** Resources. **Tae-Don Kim:** Funding acquisition. **Nak Cheol Jeong:** Conceptualization. **Sungchan Cho:** Conceptualization, Data curation, Formal analysis, Funding acquisition, Investigation, Methodology, Project administration, Supervision, Writing – review & editing.

Declaration of competing interest

The authors declare that they have no known competing financial interests or personal relationships that could have appeared to influence the work reported in this paper.

Data availability

Data will be made available on request.

Acknowledgement

This research was supported by grants from the National Research Foundation of Korea (NRF-2020R1A2C2012347 and -2022M3E5F2018457), the National Research Council of Science & Technology (NST) (CAP-18-02-KRIBB), UST Young Scientist+ Research Program 2022 through the University of Science and Technology (2022YS17), and the KRIBB Research Initiative Programs (KGM1402312 and KGM1062312).

Appendix A. Supplementary data

Supplementary data to this article can be found online at https://doi.org/10.1016/j.bios.2023.115169.

Supplementary data

Supplementary data associated with this article are published online only. To view these files, please visit the journal online.

References

Abe, K.T., Li, Z., Samson, R., Samavarchi-Tehrani, P., Valcourt, E.J., Wood, H., Budylowski, P., Dupuis, A.P., Girardin, R.C., Rathod, B., 2020. A simple protein-based surrogate neutralization assay for SARS-CoV-2. JCI Insight 5 (19).

Alves Ferreira-Bravo, I., DeStefano, J.J., 2021. Xeno-nucleic acid (XNA) 2'-fluoro-arabino nucleic acid (FANA) aptamers to the receptor-binding domain of SARS-CoV-2 S protein block ACE2 binding. Viruses 13 (10), 1983.

Alves, J., Engel, L., de Vasconcelos Cabral, R., Rodrigues, E.L., de Jesus Ribeiro, L., Higa, L.M., da Costa Ferreira Junior, O., Castineiras, T., de Carvalho Leitao, I., Tanuri, A., Goueli, S.A., Zegzouti, H., 2021. A bioluminescent and homogeneous SARS-CoV-2 spike RBD and hACE2 interaction assay for antiviral screening and monitoring patient neutralizing antibody levels. Sci. Rep. 11 (1), 18428.

Anik, M.I., Hossain, M.K., Hossain, I., Mahfuz, A., Rahman, M.T., Ahmed, I., 2021. Recent progress of magnetic nanoparticles in biomedical applications: a review. Nano Select 2 (6), 1146–1186.

Attallah, C., Etcheverrigaray, M., Kratje, R., Oggero, M., 2017. A highly efficient modified human serum albumin signal peptide to secrete proteins in cells derived from different mammalian species. Protein Expr. Purif. 132, 27–33.

Azad, T., Singaravelu, R., Brown, E.E.F., Taha, Z., Rezaei, R., Arulanandam, R., Boulton, S., Diallo, J.S., Ilkow, C.S., Bell, J.C., 2021a. SARS-CoV-2 S1 NanoBiT: a nanoluciferase complementation-based biosensor to rapidly probe SARS-CoV-2 receptor recognition. Biosens. Bioelectron. 180, 113122.

Azad, T., Singaravelu, R., Taha, Z., Jamieson, T.R., Boulton, S., Crupi, M.J., Martin, N.T., Brown, E.E., Poutou, J., Ghahremani, M., 2021b. Nanoluciferase complementation-based bioreporter reveals the importance of N-linked glycosylation of SARS-CoV-2 S for viral entry. Mol. Ther. 29 (6), 1984–2000.

Brown, E.E.F., Rezaei, R., Jamieson, T.R., Dave, J., Martin, N.T., Singaravelu, R., Crupi, M.J.F., Boulton, S., Tucker, S., Duong, J., Poutou, J., Pelin, A., Yasavoli-Sharahi, H., Taha, Z., Arulanandam, R., Surendran, A., Ghahremani, M., Austin, B., Matar, C., Diallo, J.S., Bell, J.C., Ilkow, C.S., Azad, T., 2021. Characterization of critical determinants of ACE2-SARS CoV-2 RBD interaction. Int. J. Mol. Sci. 22 (5).

Cao, L., Goreshnik, I., Coventry, B., Case, J.B., Miller, L., Kozodoy, L., Chen, R.E., Carter, L., Walls, A.C., Park, Y.-J., 2020. De novo design of picomolar SARS-CoV-2 miniprotein inhibitors. Science 370 (6515), 426–431.

Carter, L.J., Garner, L.V., Smoot, J.W., Li, Y., Zhou, Q., Saveson, C.J., Sasso, J.M., Gregg, A.C., Soares, D.J., Beskid, T.R., 2020. Assay Techniques and Test Development for COVID-19 Diagnosis. ACS Publications.

ChemAxon, 2017. Instant JChem. Version 5.6.0. Budapest, Hungary. https://chemaxon.com/.

Cho, H.J., Oh, B.M., Kim, J.-T., Lim, J., Park, S.Y., Hwang, Y.S., Baek, K.E., Kim, B.-Y., Choi, I., Lee, H.G., 2019. Efficient Interleukin-21 Production by Optimization of Codon and Signal Peptide in Chinese Hamster Ovarian Cells.

Choi, M., Kim, A.K., Ham, Y., Lee, J.Y., Kim, D., Yang, A., Jo, M.J., Yoon, E., Heo, J.N., Han, S.B., Ki, M.H., Lee, K.S., Cho, S., 2021. Aristolactam BIII, a naturally derived DYRK1A inhibitor, rescues Down syndrome-related phenotypes. Phytomedicine 92, 153695.

Fan, Y., Li, X., Zhang, L., Wan, S., Zhang, L., Zhou, F., 2022. SARS-CoV-2 Omicron variant: recent progress and future perspectives. Signal Transduct. Targeted Ther. 7 (1), 141.

Friesner, R.A., Banks, J.L., Murphy, R.B., Halgren, T.A., Klicic, J.J., Mainz, D.T., Repasky, M.P., Knoll, E.H., Shelley, M., Perry, J.K., Shaw, D.E., Francis, P., Shenkin, P.S., 2004. Glide: a new approach for rapid, accurate docking and scoring. 1. Method and assessment of docking accuracy. J. Med. Chem. 47 (7), 1739–1749.

Gattinger, P., Niespodziana, K., Stiasny, K., Sahanic, S., Tulaeva, I., Borochova, K., Dorofeeva, Y., Schlederer, T., Sonnweber, T., Hofer, G., 2022. Neutralization of SARS-CoV-2 requires antibodies against conformational receptor-binding domain epitopes. Allergy 77 (1), 230–242.

Guler-Gane, G., Kidd, S., Sridharan, S., Vaughan, T.J., Wilkinson, T.C., Tigue, N.J., 2016. Overcoming the refractory expression of secreted recombinant proteins in mammalian cells through modification of the signal peptide and adjacent amino acids. PLoS One 11 (5), e0155340.

Kim, S.J., Yao, Z., Marsh, M.C., Eckert, D.M., Kay, M.S., Lyakisheva, A., Pasic, M., Bansal, A., Birnboim, C., Jha, P., 2022. Homogeneous surrogate virus neutralization assay to rapidly assess neutralization activity of anti-SARS-CoV-2 antibodies. Nat. Commun. 13 (1), 3716.

Kober, L., Zehe, C., Bode, J., 2013. Optimized signal peptides for the development of high expressing CHO cell lines. Biotechnol. Bioeng. 110 (4), 1164–1173.

Li, Q., Wu, J., Nie, J., Zhang, L., Hao, H., Liu, S., Zhao, C., Zhang, Q., Liu, H., Nie, L., 2020. The impact of mutations in SARS-CoV-2 spike on viral infectivity and antigenicity. Cell 182 (5), 1284–1294. e1289.

Liu, H., Zou, X., Li, T., Wang, X., Yuan, W., Chen, Y., Han, W., 2016. Enhanced production of secretory glycoprotein VSTM1-v2 with mouse IgGκ signal peptide in optimized HEK293F transient transfection. J. Biosci. Bioeng. 121 (2), 133–139.

Mahmud, N., Anik, M.I., Hossain, M.K., Khan, M.I., Uddin, S., Ashrafuzzaman, M., Rahaman, M.M., 2022. Advances in nanomaterial-based platforms to combat COVID-19: diagnostics, preventions, therapeutics, and vaccine developments. ACS Appl. Bio Mater. 5 (6), 2431–2460.

Min, L., Sun, Q., 2021. Antibodies and vaccines target RBD of SARS-CoV-2. Front. Mol. Biosci. 8, 671633.

Pal, M., Berhanu, G., Desalegn, C., Kandi, V., 2020. Severe acute respiratory syndrome coronavirus-2 (SARS-CoV-2): an update. Cureus 12 (3).

Roman, R., Miret, J., Scalia, F., Casablancas, A., Lecina, M., Cairo, J.J., 2016. Enhancing heterologous protein expression and secretion in HEK293 cells by means of combination of CMV promoter and IFNalpha2 signal peptide. J. Biotechnol. 239, 57–60.

Tada, T., Zhou, H., Dcosta, B.M., Samanovic, M.I., Chivukula, V., Herati, R.S., Hubbard, S.R., Mulligan, M.J., Landau, N.R., 2022. Increased resistance of SARS-CoV-2 Omicron variant to neutralization by vaccine-elicited and therapeutic antibodies. EBioMedicine 78, 103944.

Toelzer, C., Gupta, K., Yadav, S.K., Borucu, U., Davidson, A.D., Kavanagh Williamson, M., Shoemark, D.K., Garzoni, F., Staufer, O., Milligan, R., 2020. Free fatty acid binding pocket in the locked structure of SARS-CoV-2 spike protein. Science 370 (6517), 725–730.

Varjosalo, M., Sacco, R., Stukalov, A., Van Drogen, A., Planyavsky, M., Hauri, S., Aebersold, R., Bennett, K.L., Colinge, J., Gstaiger, M., 2013. Interlaboratory reproducibility of large-scale human protein-complex analysis by standardized AP-MS. Nat. Methods 10 (4), 307–314.

Wan, J., Xing, S., Ding, L., Wang, Y., Gu, C., Wu, Y., Rong, B., Li, C., Wang, S., Chen, K., 2020. Human-IgG-neutralizing monoclonal antibodies block the SARS-CoV-2 infection. Cell Rep. 32 (3), 107918.

Wu, W., Tan, X., Zupancic, J., Schardt, J.S., Desai, A.A., Smith, M.D., Zhang, J., Xie, L., Oo, M.K., Tessier, P.M., 2022. Rapid and quantitative in vitro evaluation of SARS-CoV-2 neutralizing antibodies and nanobodies. Anal. Chem. 94 (10), 4504–4512.

Yang, X., Liu, L., Hao, Y., So, E., Emami, S.S., Zhang, D., Gong, Y., Sheth, P.M., Wang, Y., 2021. A bioluminescent biosensor for quantifying the interaction of SARS-CoV-2 and its receptor ACE2 in cells and in vitro. Viruses 13 (6).